

# RSC Advances



This is an *Accepted Manuscript*, which has been through the Royal Society of Chemistry peer review process and has been accepted for publication.

*Accepted Manuscripts* are published online shortly after acceptance, before technical editing, formatting and proof reading. Using this free service, authors can make their results available to the community, in citable form, before we publish the edited article. This *Accepted Manuscript* will be replaced by the edited, formatted and paginated article as soon as this is available.

You can find more information about *Accepted Manuscripts* in the [Information for Authors](#).

Please note that technical editing may introduce minor changes to the text and/or graphics, which may alter content. The journal's standard [Terms & Conditions](#) and the [Ethical guidelines](#) still apply. In no event shall the Royal Society of Chemistry be held responsible for any errors or omissions in this *Accepted Manuscript* or any consequences arising from the use of any information it contains.



## Adhesive RAFT Agents for Controlled Polymerization of Acrylamide: Effect of Catechol-end R Groups†

Olabode Oyeneye, William Z. Xu and Paul A. Charpentier\*

Received 00th January 20xx,  
Accepted 00th January 20xx

DOI: 10.1039/x0xx00000x

www.rsc.org/

Synthesizing polyacrylamide (PAM) inorganic nanocomposites with stable tethering and controlled polymer length has been elusive. Herein, we report on the synthesis of trithiocarbonates with several catechol end R groups (as anchors) that differ in their carbonyl  $\alpha$ -substituents. These so-called adhesive RAFT agents were subsequently examined in batch RAFT polymerization of acrylamide (AM) monomer to study their livingness characteristics. The catechol-end trithiocarbonates' (Dopa-CTAs) and catechol-end PAM structures ( $\leq 46$  kDa) were confirmed via 1D ( $^1\text{H}$  and  $^{13}\text{C}$ ) and 2D (gHSQC, gHMBC) NMR. Subsequent anchoring of the end-functionalized PAM (*grafting to*) via catechol induced linkage to  $\gamma$ -alumina nanoparticles was successful, giving good correlation based on ATR-FTIR, DLS and TGA analyses. This unique methodology enables PAM-inorganic nanocomposites to be synthesized with stable tethering without significant rate retardation.

### 1 Introduction

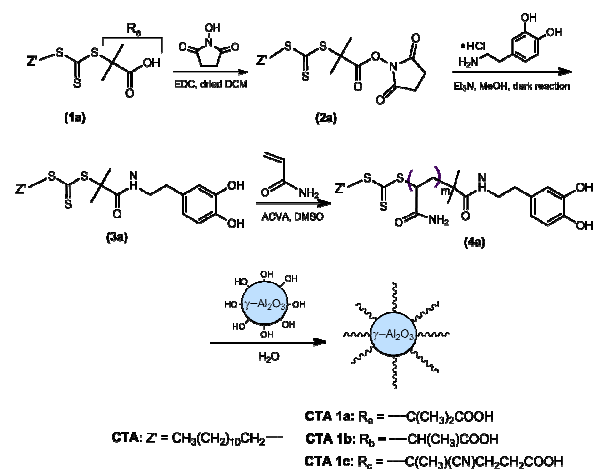
Polymeric inorganic nanocomposites (PNCs) using so-called "smart" (co)polymers<sup>1-4</sup> have shown potential by harnessing the synergic effects of both the polymer and inorganic components to enhance properties for end-use applications such as water treatment flocculation.<sup>5-7</sup> For linking the polymer component to inorganic nanoparticles, various coupling molecules have been investigated including carboxyls,<sup>8</sup> catechol derivatives,<sup>9-13</sup> phosph(on)ates,<sup>14</sup> silanes,<sup>15-17</sup> and thiols.<sup>18-20</sup> Catechol derivatives have been shown to provide strong and stable chemisorption bonding between the polymer component and inorganic nanoparticles.<sup>11-13</sup> To provide this catechol functionality, dopamine is bifunctional with an amine moiety that can be chemically modified for amide linkage formation to polymer while the catechol will promote mono- or bi-dentate bonding to the inorganic nanoparticles (NPs).<sup>21,22</sup> Strategies commonly used for the synthesis of pre-defined PNCs involve controlled radical polymerization (CRP) using either "grafting from" or "grafting to" approaches, with the latter entailing the immobilization of end-functionalized polymer on NPs. The inorganic NPs being the core help define the final morphology of the PNC, in conjunction with controlled polymerization to ensure uniform extension of the polymeric chains from the NP core. Of the CRP techniques, the reversible addition-fragmentation chain transfer (RAFT) polymerization method has been given immense attention for the synthesis of advanced materials. This is because of

potential for tailored materials with predetermined molecular weight (MW), complex architectures, diverse functionalities and narrow dispersity ( $\text{Đ}$ ).<sup>23</sup> In particular, the RAFT polymerization technique has been shown to possess advantages over both ATRP and nitroxide techniques because of the ease of implementation and the wide range of applicable monomers (functional and non-functional), solvents and conditions. Under the "grafting to" approach, end-functionalized polymers can be prepared utilizing a RAFT agent (ZC(=S)SR) that has a Z- or R- substituent bearing the required end-group.<sup>8,24</sup> However, selection of the substituents needs to be suited for the specific monomer, as they influence the RAFT agent reactivity, solubility and polymerization kinetics.<sup>25</sup> Among the various classes of RAFT agents, trithiocarbonates are more hydrolytically stable and offer better control over polymer structure derived from more activated monomers, such as acrylamide.<sup>26</sup> A number of studies have utilized a catechol moiety (as an adhesive molecule) with RAFT polymerization techniques for PNC syntheses, and catechol end-functionalization of polymers is often achieved in-situ using catechol bearing RAFT agents for polymerization<sup>13,27</sup> or after polymer synthesis via post-modification.<sup>28,29</sup> However, to the best of our knowledge, no studies have attempted to compare catechol bearing RAFT agents having differing substituents at their alpha positions for the most suited livingness characteristics with respect to monomers. Herein, we investigate the influence of trithiocarbonate RAFT agents bearing the same Z group but different catechol end R groups on acrylamide (AM) polymerization, and subsequent anchoring of the resulting polymer to  $\gamma$ -alumina NPs. More specifically, the catechol RAFT agents differ in the substituents on their trithiocarbonate  $\alpha$  carbon, and one of the RAFT agents being more bulky (see Scheme 1). The catechol end R group affects the partitioning of

Department of Chemical and Biochemical Engineering, University of Western Ontario, London ON, N6A 5B9, Canada.  
E-mail: pcharpentier@eng.uwo.ca

† Electronic Supplementary Information (ESI) available: Complementary experimental section, NMR, ATR-FTIR and UV-vis spectra; polymerization kinetic plots; and in-situ NMR polymerization spectra. See DOI: 10.1039/x0xx00000x

63 intermediate radicals, and should be a good homolytic leaving  
64 group for preferential partitioning into new radical species  
65 (derived from the R-group) which are capable of efficient re-  
66 initiation.<sup>30,31</sup> We focused on end-functionalized polymers for  
67 subsequent "grafting to" as opposed to surface-initiated  
68 polymerization, because dense anchoring of the catechol-  
69 CTA on metal oxide NPs requires conditions that call for  
70 hydrolytic decomposition of trithiocarbonate groups.<sup>10,32</sup>  
71 AM monomer was chosen because of the wide utility of PAA  
72 in applications as flocculants or additives in wastewater  
73 treatment,<sup>5,33,34</sup> while  $\gamma$ -Al<sub>2</sub>O<sub>3</sub> was employed because of its  
74 high OH density, high surface activity and propensity for  
75 wastewater treatment.<sup>35,36</sup>



**Scheme 1.** End-functionalization of polyacrylamide with RAFT agents possessing different catechol-end R groups

## 76 Experimental Section

77 **Materials:**  $\gamma$ -alumina ( $d_{TEM} \leq 50$  nm, surface area  $> 40$  m<sup>2</sup>/g  
78 (BET), acrylamide (AM,  $\geq 98\%$ ), 4,4'-azobis(4-cyanovaleic acid)  
79 (ACVA,  $\geq 98\%$ ), Dopamine hydrochloride, hydroxysuccinimide (NHS, 98%),  
80 *N*-(3-dimethylaminopropyl) carbodiimide hydrochloride (EDC,  $\geq 98\%$ ), sodium  
81 chloride (NaCl,  $\geq 99\%$ ), 2-(dodecylthiocarbonothioylthio) methylpropionic  
82 acid (DDMAT, 98%), dodecylthiocarbonothioylthio propionic acid (DoPAT, 97%),  
83 cyano-4-[(dodecylsulfanylthiocarbonyl)sulfanyl]pentanoic acid (CDSPA, 97%)  
84 and methanol (MeOH,  $\geq 99.9\%$ ) were purchased from Sigma Aldrich, Canada  
85 and used as received. All other organic solvents used were the highest purity available from the  
86 Caledon Laboratory Ltd., Canada. Sodium bicarbonate (NaHCO<sub>3</sub>,  $\geq 95\%$ ),  
87 anhydrous sodium sulfate (Na<sub>2</sub>SO<sub>4</sub>,  $\geq 99\%$ ) and anhydrous magnesium sulfate  
88 (MgSO<sub>4</sub>) and sulfuric acid (96.5%) were obtained from the Caledon Labs  
89 (Canada). Triethylamine (Et<sub>3</sub>N, 99.5%) and hydrogen peroxide (30%) were  
90 procured from EDM Chemicals (USA). Dialysis membranes (5000 Da) and  
91 3,500 Da) were purchased from Spectrum Laboratories, Inc. while 25  $\mu$ m  
92 filters (Fischer Scientific) were obtained from VWR Canada. All batch  
93 polymerization reactions were

previously purged under argon atmosphere (ultra-high purity, Praxair Inc. Canada).

**Characterization:** A brief and detailed description of the characterization methods can be found in the ESI.†

**Synthesis of RAFT Agents with (2,5-dioxopyrrolidin-1-yl)oxidanyl End Groups (Suc-CTAs, (2a-c)):** The synthesis of Suc-CTAs was performed based on a literature method<sup>13</sup> by varying R groups while using a simplified workup procedure. NHS (0.40 g, 3.40mmol) and EDC (0.76 g, 3.43mmol) were added to 2.68mmol each of CDSPA, DDMAT, and DoPAT dissolved in dried DCM (30 mL, previously dried with anhydrous Na<sub>2</sub>SO<sub>4</sub>), and allowed to react for 18 hr under continuous stirring at room temperature. Each reaction mixture was then washed with 150 mL of saturated NaHCO<sub>3</sub> (aq) before collecting the DCM phase. Further extraction from the aqueous phase was carried out with ethyl ether (5x30 mL), and then combined with the DCM phase to give a single organic phase, which was washed with deionized water (3x50 mL), brine (3x50 mL) and dried over anhydrous MgSO<sub>4</sub> (7.0 g). The hydrated MgSO<sub>4</sub> was filtered off and the solvent removed using a Rotavap to obtain yellowish solid products.

Suc-DDMAT: <sup>1</sup>H NMR (600 MHz, CDCl<sub>3</sub>)  $\delta$  (ppm): 0.89 (t,  $J = 7.0$  Hz, 3 H, CH<sub>3</sub>CH<sub>2</sub>CH<sub>2</sub>), 1.23 - 1.34 (m, 16 H, CH<sub>3</sub>(CH<sub>2</sub>)<sub>8</sub>CH<sub>2</sub>), 1.36 - 1.42 (m, 2 H, CH<sub>2</sub>(CH<sub>2</sub>)<sub>2</sub>S), 1.66 - 1.72 (m, 2 H, CH<sub>2</sub>CH<sub>2</sub>S), 1.88 (s, 6 H, C(CH<sub>3</sub>)<sub>2</sub>), 2.82 (m, 4 H, (O=C)CH<sub>2</sub>C(=O)), 3.31 (t,  $J = 7.0$  Hz, 2 H, CH<sub>2</sub>S); <sup>13</sup>C NMR (100 MHz, CDCl<sub>3</sub>)  $\delta$  (ppm): 14.1 (CH<sub>3</sub>CH<sub>2</sub>CH<sub>2</sub>), 22.7 (CH<sub>3</sub>CH<sub>2</sub>CH<sub>2</sub>), 25.6 (C(CH<sub>3</sub>)<sub>2</sub>, (O=C)CH<sub>2</sub>C(=O)), 27.8 (CH<sub>2</sub>CH<sub>2</sub>S), 29.0 (CH<sub>2</sub>(CH<sub>2</sub>)<sub>2</sub>S), 29.1(CH<sub>2</sub>(CH<sub>2</sub>)<sub>3</sub>S), 29.3 (CH<sub>2</sub>(CH<sub>2</sub>)<sub>4</sub>S), 29.4 (CH<sub>3</sub>(CH<sub>2</sub>)<sub>2</sub>CH<sub>2</sub>), 29.5 (CH<sub>3</sub>(CH<sub>2</sub>)<sub>2</sub>CH<sub>2</sub>), 29.6 (CH<sub>3</sub>(CH<sub>2</sub>)<sub>4</sub>(CH<sub>2</sub>)<sub>2</sub>), 31.9 (CH<sub>3</sub>CH<sub>2</sub>CH<sub>2</sub>), 37.2 (CH<sub>2</sub>CH<sub>2</sub>S), 54.3 (C(CH<sub>3</sub>)<sub>2</sub>), 168.6 (N(C=O)<sub>2</sub>), 169.1 (C(=O)O), 218.7 (SC(=S)S). FTIR (cm<sup>-1</sup>): 2916 ( $\nu_{as}$ CH<sub>2</sub>), 2847 ( $\nu_s$ CH<sub>2</sub>), 1777 ( $\nu$ C=O, imide), 1734 ( $\nu$ C=O, ester), 1202 ( $\nu$ C-O, ester), 1073 ( $\nu$ C=S), 811( $\nu_{as}$ S-C-S).

Suc-DoPAT: <sup>1</sup>H NMR (600 MHz, CDCl<sub>3</sub>)  $\delta$  (ppm): 0.88 (t,  $J = 7.0$  Hz, 3 H, CH<sub>3</sub>CH<sub>2</sub>CH<sub>2</sub>), 1.22 - 1.33 (m, 16 H, CH<sub>3</sub>(CH<sub>2</sub>)<sub>8</sub>CH<sub>2</sub>), 1.39 (quin,  $J = 7.2$  Hz, 2 H, CH<sub>2</sub>(CH<sub>2</sub>)<sub>2</sub>S), 1.62 - 1.73 (m, 2 H, CH<sub>2</sub>CH<sub>2</sub>S), 1.75 (d,  $J = 7.4$  Hz, 3 H, CH(CH<sub>3</sub>)), 2.83 (br. s, 4 H, (O=C)CH<sub>2</sub>C(=O)), 3.37 (td,  $J = 7.4$  Hz  $\times$  2 and 3.1 Hz, 2 H, CH<sub>2</sub>S), 5.14 (q,  $J = 7.4$  Hz, 1 H, CH(CH<sub>3</sub>)); <sup>13</sup>C NMR (100 MHz, CDCl<sub>3</sub>)  $\delta$  (ppm): 14.1 (CH<sub>3</sub>CH<sub>2</sub>CH<sub>2</sub>), 16.7 (CH(CH<sub>3</sub>)), 22.6 (CH<sub>3</sub>CH<sub>2</sub>CH<sub>2</sub>), 25.6 ((O=C)CH<sub>2</sub>C(=O)), 27.8 (CH<sub>2</sub>CH<sub>2</sub>S), 28.9 (CH<sub>2</sub>(CH<sub>2</sub>)<sub>2</sub>S), 29.0 (CH<sub>2</sub>(CH<sub>2</sub>)<sub>3</sub>S), 29.3 (CH<sub>2</sub>(CH<sub>2</sub>)<sub>4</sub>S), 29.4 (CH<sub>3</sub>(CH<sub>2</sub>)<sub>2</sub>CH<sub>2</sub>), 29.5 (CH<sub>3</sub>(CH<sub>2</sub>)<sub>2</sub>CH<sub>2</sub>), 29.6 (CH<sub>3</sub>(CH<sub>2</sub>)<sub>4</sub>(CH<sub>2</sub>)<sub>2</sub>), 31.9 (CH<sub>3</sub>CH<sub>2</sub>CH<sub>2</sub>), 37.5 (CH<sub>2</sub>CH<sub>2</sub>S), 45.0 (CH(CH<sub>3</sub>)), 167.2 (N(C=O)<sub>2</sub>), 168.5 (C(=O)O), 220.2 (SC(=S)S). FTIR (cm<sup>-1</sup>): 2914 ( $\nu_{as}$ CH<sub>2</sub>), 2848 ( $\nu_s$ CH<sub>2</sub>), 1786 ( $\nu$ C=O, imide), 1736 ( $\nu$ C=O, ester), 1471, 1358, 1200 ( $\nu$ C-O, ester), 1073 ( $\nu$ C=S), 813( $\nu_{as}$ S-C-S).

Suc-CDSPA: <sup>1</sup>H NMR (600 MHz, CDCl<sub>3</sub>)  $\delta$  (ppm): 0.89 (t,  $J = 7.0$  Hz, 3 H, CH<sub>3</sub>CH<sub>2</sub>CH<sub>2</sub>), 1.23 - 1.33 (m, 16 H, CH<sub>3</sub>(CH<sub>2</sub>)<sub>8</sub>CH<sub>2</sub>), 1.35 - 1.44 (m, 2 H, CH<sub>2</sub>(CH<sub>2</sub>)<sub>2</sub>S), 1.66 - 1.73 (m, 2 H, CH<sub>2</sub>CH<sub>2</sub>S), 1.89 (s, 3 H, C(CH<sub>3</sub>)), 2.48 - 2.69 (m, 2 H, CH<sub>2</sub>CH<sub>2</sub>C(=O)O), 2.85 (br. s, 4 H, (O=C)CH<sub>2</sub>C(=O)), 2.94 (ddd,  $J = 10.0, 6.2, 3.8$  Hz, 2 H, CH<sub>2</sub>C(=O)O), 3.34 (t,  $J = 7.3$  Hz, 2 H, CH<sub>2</sub>CH<sub>2</sub>S); <sup>13</sup>C NMR (100 MHz, CDCl<sub>3</sub>)  $\delta$  (ppm): 14.1 (CH<sub>3</sub>CH<sub>2</sub>CH<sub>2</sub>), 22.7 (CH<sub>3</sub>CH<sub>2</sub>CH<sub>2</sub>), 24.8 (C(CH<sub>3</sub>)), 25.6 ((O=C)CH<sub>2</sub>C(=O)), 26.8 (CH<sub>2</sub>C(=O)O), 27.6

- 154 (CH<sub>2</sub>CH<sub>2</sub>S), 28.9 (CH<sub>2</sub>(CH<sub>2</sub>)<sub>2</sub>S), 29.0 (CH<sub>2</sub>(CH<sub>2</sub>)<sub>3</sub>S), 29.1 (CH<sub>2</sub>(CH<sub>2</sub>)<sub>4</sub>S), 29.4 (CH<sub>3</sub>(CH<sub>2</sub>)<sub>2</sub>CH<sub>2</sub>), 29.5 (CH<sub>3</sub>(CH<sub>2</sub>)<sub>3</sub>CH<sub>2</sub>), 29.6 (CH<sub>3</sub>(CH<sub>2</sub>)<sub>4</sub>CH<sub>2</sub>), 31.9 (CH<sub>3</sub>CH<sub>2</sub>CH<sub>2</sub>), 33.2 (CH<sub>2</sub>CH<sub>2</sub>C(=O)NH), 37.1 (CH<sub>2</sub>CH<sub>2</sub>S), 46.0 ((CH<sub>3</sub>)C(C≡N)), 118.6 (C(C≡N)), 162.1 (C(=O)O), 168.8 (N(C=O)<sub>2</sub>), 216.5 (SC(=S)S). FTIR (cm<sup>-1</sup>): 2814 (ν<sub>as</sub>CH<sub>2</sub>), 2848 (ν<sub>s</sub>CH<sub>2</sub>), 2235 (νC≡N), 1820, 1783 (νC=O, imide), 1734 (νC=O, ester), 1423, 1383, 1293, 1199 (νC-O, ester), 1066 (νC=S), 884, 803 (ν<sub>as</sub>S-C-S).
- 162 **Synthesis of Catechol End Group CTAs (Dopa-CTAs (3a-c))**  
 163 Typically, dopamine hydrochloride (0.50 g, 2.64 mmol) and  
 164 each of Suc-CDSPA, Suc-DDMAT and Suc-DoPAT (2.13 mmol)  
 165 were added to MeOH (30 mL) with Et<sub>3</sub>N (0.40 mL, 2.87 mmol)  
 166 and allowed to undergo dark reaction for 48 hr at room  
 167 temperature under continuous stirring. At the end of the  
 168 reaction, the solvent was removed by rotary evaporation,  
 169 followed by the addition of ether (20 mL) and washing of the  
 170 aqueous phase. Subsequently, the ether phase was washed  
 171 with deionized water (3×15 mL) and brine (3×15 mL). The  
 172 ether solvent was removed by vacuum evaporation, and then  
 173 the viscous solute cooled (4°C) before precipitating in hexane  
 174 (except for Dopa-CDSPA) to give a bright yellow solid product  
 175 which was vacuum dried. In the case of Dopa-CDSPA, further  
 176 purification was carried out via preparative column  
 177 chromatography using silica gel (ethyl acetate: hexane =  
 178 v/v).  
 179 Dopa-DDMAT: <sup>1</sup>H NMR (600 MHz, CDCl<sub>3</sub>) δ (ppm): 0.89 (t, J=7.0  
 180 Hz, 3 H, CH<sub>3</sub>CH<sub>2</sub>CH<sub>2</sub>), 1.23- 1.32 (m, 16 H, CH<sub>3</sub>(CH<sub>2</sub>)<sub>8</sub>CH<sub>2</sub>), 1.36-  
 181 1.41 (m, 2 H, CH<sub>2</sub>(CH<sub>2</sub>)<sub>2</sub>S), 1.66 (s, 8 H, CH<sub>2</sub>CH<sub>2</sub>S, C(CH<sub>3</sub>)<sub>2</sub>), 2.57  
 182 (t, J=7.0 Hz, 2 H, CH<sub>2</sub>-ArC), 3.26 (t, J=7.6 Hz, 2 H, CH<sub>2</sub>CH<sub>2</sub>S),  
 183 3.41-3.49 (m, 2 H, NHCH<sub>2</sub>CH<sub>2</sub>), 6.56 (dd, J=8.0, 2.2 Hz, 1 H, ArC-  
 184 H(m-OH)), 6.64 (t, J=5.5 Hz, 1 H, NHCH<sub>2</sub>CH<sub>2</sub>), 6.71 (d, J=2.0 Hz,  
 185 1 H, ArC-H(o-OH)), 6.80 (d, J=8.2 Hz, 1 H, ArC-H(o-OH)); <sup>13</sup>C  
 186 NMR (100 MHz, CDCl<sub>3</sub>) δ (ppm): 14.1 (CH<sub>3</sub>CH<sub>2</sub>CH<sub>2</sub>), 22.7  
 187 (CH<sub>3</sub>CH<sub>2</sub>CH<sub>2</sub>), 25.8 (C(CH<sub>3</sub>)<sub>2</sub>), 27.7 (CH<sub>2</sub>CH<sub>2</sub>S), 29.0 (CH<sub>2</sub>(CH<sub>2</sub>)<sub>3</sub>S),  
 188 29.1 (CH<sub>2</sub>(CH<sub>2</sub>)<sub>3</sub>S), 29.3 (CH<sub>2</sub>(CH<sub>2</sub>)<sub>4</sub>S), 29.4 (CH<sub>3</sub>(CH<sub>2</sub>)<sub>2</sub>CH<sub>2</sub>),  
 189 (CH<sub>3</sub>(CH<sub>2</sub>)<sub>3</sub>CH<sub>2</sub>), 29.6 (CH<sub>3</sub>(CH<sub>2</sub>)<sub>4</sub>(CH<sub>2</sub>)<sub>2</sub>), 31.9 (CH<sub>3</sub>CH<sub>2</sub>CH<sub>2</sub>),  
 190 (NHCH<sub>2</sub>CH<sub>2</sub>), 37.2 (CH<sub>2</sub>CH<sub>2</sub>S), 41.7 (NHCH<sub>2</sub>CH<sub>2</sub>), 57.1 (C(CH<sub>3</sub>)<sub>2</sub>),  
 191 115.2 (ArC-H(o-OH)), 115.4 (ArC-H(o-OH)), 120.8 (ArC-H(o-OH)),  
 192 130.8 (CH<sub>2</sub>-ArC), 142.9 (ArC-OH), 144.0 (ArC-OH), 172.8  
 193 (CC(=O)NH), 219.9 (SC(=S)S). FTIR (cm<sup>-1</sup>): 3340 (νNH, amide I),  
 194 3186 (νOH, phenol), 2920 (ν<sub>as</sub>CH<sub>2</sub>), 2850 (ν<sub>s</sub>CH<sub>2</sub>), 1622 (νC=O,  
 195 1604 (νC=O, amide I & νC=C, aromatic), 1531 (νC-N & δNH,  
 196 amide II), 1447, 1361, 1291, 1252, 1158, 1112, 1072 (νC-S),  
 197 813 (ν<sub>as</sub>S-C-S).  
 198 Dopa-DoPAT: <sup>1</sup>H NMR (600 MHz, CDCl<sub>3</sub>) δ (ppm): 0.89 (t, J=7.0  
 199 Hz, 3 H, CH<sub>3</sub>CH<sub>2</sub>CH<sub>2</sub>), 1.21 - 1.35 (m, 16 H, CH<sub>3</sub>(CH<sub>2</sub>)<sub>8</sub>CH<sub>2</sub>), 1.36-  
 200 1.45 (m, 2 H, CH<sub>2</sub>(CH<sub>2</sub>)<sub>2</sub>S), 1.55 (d, J=7.6 Hz, 3 H, CH(CH<sub>3</sub>)), 2.57  
 201 (quin, J=7.5 Hz, 2 H, CH<sub>2</sub>CH<sub>2</sub>S), 2.66 (t, J=6.8 Hz, 2 H, CH<sub>2</sub>-ArC),  
 202 3.28 - 3.49 (m, 4 H, CH<sub>2</sub>CH<sub>2</sub>S, NHCH<sub>2</sub>CH<sub>2</sub>), 4.69 (q, J=7.6 Hz, 2 H,  
 203 CH(CH<sub>3</sub>)), 6.50 (t, J=5.6 Hz, 1 H, NHCH<sub>2</sub>CH<sub>2</sub>), 6.57 (dd, J=7.9,  
 204 Hz, 1 H, ArC-H(m-OH)), 6.67 (d, J=1.8 Hz, 1 H, ArC-H(o-OH)),  
 205 6.80 (d, J=8.2 Hz, 1 H, ArC-H(o-OH)); <sup>13</sup>C NMR (600 MHz, DMF-  
 206 d<sub>6</sub>) δ (ppm): 0.83 (t, J=6.8 Hz, 3 H, CH<sub>3</sub>CH<sub>2</sub>CH<sub>2</sub>), 1.16 - 1.27 (m,  
 207 16 H, CH<sub>3</sub>(CH<sub>2</sub>)<sub>8</sub>CH<sub>2</sub>), 1.28 - 1.35 (m, 2 H, CH<sub>2</sub>(CH<sub>2</sub>)<sub>2</sub>S), 1.42 (m,  
 208 J=7.0 Hz, 3 H, CH(CH<sub>3</sub>)), 1.60 (quin, J=7.5 Hz, 2 H, CH<sub>2</sub>CH<sub>2</sub>S),  
 209 2.48 (m, 2 H, CH<sub>2</sub>-ArC), 3.10 - 3.22 (m, 2 H, NHCH<sub>2</sub>CH<sub>2</sub>), 3.33 (q,  
 J=7.6 Hz, 2 H, CH<sub>2</sub>CH<sub>2</sub>S), 4.64 (q, J=7.0 Hz, 1 H, CH(CH<sub>3</sub>)), 6.39  
 (dd, J=7.9, 2.1 Hz, 1 H, ArC-H(m-OH)), 6.54 (d, J=2.4 Hz, 1 H,  
 ArC-H(o-OH)), 6.59 (d, J=7.6 Hz, 1 H, ArC-H(o-OH)); 8.60 (s) &  
 8.69 (s) (2H, Ar-OH), 8.31 (t, J=5.6 Hz, 1 H, NHCH<sub>2</sub>CH<sub>2</sub>); <sup>13</sup>C NMR  
 (100 MHz, CDCl<sub>3</sub>) δ (ppm): 14.1 (CH<sub>3</sub>CH<sub>2</sub>CH<sub>2</sub>), 16.1 (CH(CH<sub>3</sub>)),  
 22.7 (CH<sub>3</sub>CH<sub>2</sub>CH<sub>2</sub>), 27.8 (CH<sub>2</sub>CH<sub>2</sub>S), 28.9 (CH<sub>2</sub>(CH<sub>2</sub>)<sub>2</sub>S), 29.1  
 (CH<sub>2</sub>(CH<sub>2</sub>)<sub>3</sub>S), 29.3 (CH<sub>2</sub>(CH<sub>2</sub>)<sub>4</sub>S), 29.4 (CH<sub>3</sub>(CH<sub>2</sub>)<sub>2</sub>CH<sub>2</sub>), 29.5  
 (CH<sub>3</sub>(CH<sub>2</sub>)<sub>3</sub>CH<sub>2</sub>), 29.6 (CH<sub>3</sub>(CH<sub>2</sub>)<sub>4</sub>(CH<sub>2</sub>)<sub>2</sub>), 31.9 (CH<sub>3</sub>CH<sub>2</sub>CH<sub>2</sub>), 34.6  
 (NHCH<sub>2</sub>CH<sub>2</sub>), 37.7 (CH<sub>2</sub>CH<sub>2</sub>S), 41.3 (NHCH<sub>2</sub>CH<sub>2</sub>), 47.8 (CH(CH<sub>3</sub>)),  
 115.3 (ArC-H(o-OH)), 115.5 (ArC-H(o-OH)), 120.7 (ArC-H(m-  
 OH)), 130.4 (CH<sub>2</sub>-ArC), 142.9 (ArC-OH), 144.0 (ArC-OH), 171.4  
 (CHC(=O)NH), 223.4 (SC(=S)S). FTIR (cm<sup>-1</sup>): 3341 (νNH, amide),  
 3238 (νOH, phenol), 2922 (ν<sub>as</sub>CH<sub>2</sub>), 2848 (ν<sub>s</sub>CH<sub>2</sub>), 1633 and  
 1616 (νC=O, amide I & νC=C, aromatic), 1522 (νC-N & δNH,  
 amide II), 1465, 1365, 1281, 1193, 1070 (νC=S), 813 (ν<sub>as</sub>S-C-S).  
 Dopa-CDSPA: <sup>1</sup>H NMR (600 MHz, CDCl<sub>3</sub>) δ (ppm): 0.89 (t, J=6.8  
 Hz, 3 H, CH<sub>3</sub>CH<sub>2</sub>CH<sub>2</sub>), 1.22 - 1.34 (m, 16 H, CH<sub>3</sub>(CH<sub>2</sub>)<sub>8</sub>CH<sub>2</sub>), 1.35 -  
 1.45 (m, 2 H, CH<sub>2</sub>(CH<sub>2</sub>)<sub>2</sub>S), 1.69 (quin, J=7.5 Hz, 2 H, CH<sub>2</sub>CH<sub>2</sub>S),  
 1.88 (s, 3 H, C(CH<sub>3</sub>)), 2.32 - 2.39 (m, 1 H, CH<sub>2</sub><sup>a</sup>CH<sub>2</sub>C(=O)), 2.42 -  
 2.47 (m, 2 H, CH<sub>2</sub>CH<sub>2</sub>C(=O)), 2.48 - 2.55 (m, 1 H, CH<sub>2</sub><sup>b</sup>CH<sub>2</sub>C(=O)),  
 2.71 (t, J=7.0 Hz, 2 H, CH<sub>2</sub>-ArC), 3.33 (t, J=7.5 Hz, 2 H, CH<sub>2</sub>CH<sub>2</sub>S),  
 3.43 - 3.54 (m, 2 H, NHCH<sub>2</sub>CH<sub>2</sub>), 5.63 (t, J=5.9 Hz, 1 H,  
 NHCH<sub>2</sub>CH<sub>2</sub>), 6.61 (dd, J=8.2, 1.7 Hz, 1 H, ArC-H(m-OH)), 6.72 (d,  
 J=1.8 Hz, 1 H, ArC-H(o-OH)), 6.83 (d, J=8.2 Hz, 1 H, ArC-H(o-  
 OH)); <sup>13</sup>C NMR (100 MHz, CDCl<sub>3</sub>) δ (ppm): 14.1 (CH<sub>3</sub>CH<sub>2</sub>CH<sub>2</sub>),  
 22.7 (CH<sub>3</sub>CH<sub>2</sub>CH<sub>2</sub>), 24.8 (C(CH<sub>3</sub>)), 27.7 (CH<sub>2</sub>CH<sub>2</sub>S), 29.0  
 (CH<sub>2</sub>(CH<sub>2</sub>)<sub>2</sub>S), 29.1 (CH<sub>2</sub>(CH<sub>2</sub>)<sub>3</sub>S), 29.3 (CH<sub>2</sub>(CH<sub>2</sub>)<sub>4</sub>S), 29.4  
 (CH<sub>3</sub>(CH<sub>2</sub>)<sub>2</sub>CH<sub>2</sub>), 29.5 (CH<sub>3</sub>(CH<sub>2</sub>)<sub>3</sub>CH<sub>2</sub>), 29.6 (CH<sub>3</sub>(CH<sub>2</sub>)<sub>4</sub>(CH<sub>2</sub>)<sub>2</sub>),  
 31.9 (CH<sub>3</sub>CH<sub>2</sub>CH<sub>2</sub>, CH<sub>2</sub>C(=O)NH), 34.5 (CH<sub>2</sub>CH<sub>2</sub>C(=O)), 34.6  
 (NHCH<sub>2</sub>CH<sub>2</sub>), 37.1 (CH<sub>2</sub>CH<sub>2</sub>S), 41.2 (NHCH<sub>2</sub>CH<sub>2</sub>), 46.6  
 ((CH<sub>3</sub>)C(C≡N)), 119.2 (C(C≡N)), 115.5 (ArC-H(o-OH)), 115.7 (ArC-  
 H(o-OH)), 120.8 (ArC-H(m-OH)), 130.7 (CH<sub>2</sub>-ArC), 142.9 (ArC-  
 OH), 144.1 (ArC-OH), 171.4 (CH<sub>2</sub>C(=O)NH), 217.2 (SC(=S)S). FTIR  
 (cm<sup>-1</sup>): 3286 (overlap: νNH, amide & νOH, phenol), 2919  
 (ν<sub>as</sub>CH<sub>2</sub>), 2851 (ν<sub>s</sub>CH<sub>2</sub>), 2233 (νC≡N), 1640 and 1603 (νC=O,  
 amide I & νC=C, aromatic), 1519 (νC-N & δNH, amide II), 1442,  
 1360, 1280, 1193, 1151, 1112, 1065 (νC=S), 803 (ν<sub>as</sub>S-C-S).
- RAFT Polymerization of Acrylamide:** All polymerization  
 experiments were performed at 2M monomer concentration  
 ([M]<sub>0</sub> = 0.049 mol AM) in 24.5 mL DMSO/DMF (97:3, vol%)  
 solvent (vol. of DMF is equivalent to 0.2[AM]<sub>0</sub>) and 70°C under  
 argon atmosphere. The DMF was added as an internal  
 reference for the determination of conversion of monomer  
 using subsequent NMR analysis. The initial CTA to initiator  
 ratio ([CTA]<sub>0</sub>/[I]<sub>0</sub> = 5) and the initial monomer to CTA ratio  
 ([M]<sub>0</sub>/[CTA]<sub>0</sub> = 500) were held constant to ensure controlled  
 polymerization. AM (3.554 g, 0.049 mol), ACVA (5.6 mg, 0.0196  
 mmol), 24.5 mL DMSO/DMF (97:3 vol%) solvent and the  
 catechol-end RAFT agent (0.098 mmol each, 3a-c) were added  
 to a 100-mL two-neck round-bottom flask equipped with a  
 magnetic stirrer, and a reflux condenser was connected to one  
 of its necks. The flask had its other neck sealed with a rubber  
 septum through which its content was purged with argon for  
 20 min, before immersing the flask into an oil bath for  
 temperature control as the experiment commenced. At  
 predetermined intervals, 2-3 drops of samples were taken for

266 monomer conversion analysis by  $^1\text{H}$  NMR while aliquots were  
 267 samples were quenched immediately in liquid nitrogen and  
 268 then purified prior to GPC analysis. The polymer samples were  
 269 purified by three cycles of precipitating in 20 times acetone  
 270 and re-dissolving in deionized  $\text{H}_2\text{O}$  before freeze-drying to  
 271 obtain dried polymer. However, for NMR analysis of the  
 272 structure of the synthesized polymer, further purification by  
 273 dialysis (3500 MWCO) against distilled water was carried out.

274 **Pre-treatment of  $\gamma\text{-Al}_2\text{O}_3$  NP:** Alumina NPs were pretreated by  
 275 washing with acetone (twice) and immersed in piranha  
 276 solution for 30 min (96.5%  $\text{H}_2\text{SO}_4$  and 30.5%  $\text{H}_2\text{O}_2$  (4:1 vol.)) to  
 277 remove organic contaminants and to enhance the  
 278 hydroxylation of the NP surface. Then, the NPs were extracted  
 279 by washing with water and ethanol, and then vacuum dried.

280 **Preparation of  $\gamma\text{-Al}_2\text{O}_3$ -PAM Nanocomposite (Al-PAM):**  
 281 Following ultrasonication of the pretreated alumina NP core  
 282 (30 mg), a solution containing (5 mg/mL) of Dopa-PAM ( $M_n =$   
 283 26500, 42600, 53800 g/mol; synthesized from Dopa-CTA (**3a**))  
 284 was dispersed in 15 mL deionized water at  $50^\circ\text{C}$  for 24 hr. The  
 285 excessive polymer was removed via dissolution and  
 286 centrifugation before freeze-drying to obtain the dried Al-PAM  
 287 nanocomposites. For preparing the control Al-PAM sample, a  
 288 similar procedure was employed except that the polymer used  
 289 was a PAM synthesized with CTA (**1a**) (without catechol  
 290 moiety,  $M_n = 29600$  g/mol).

## 291 Results & Discussion

292 **Synthesis and Characteristics of Catechol End Group RAFT Agents**  
 293 **(Dopa-CTAs (**3a-c**)):** Though the carboxyl group of the CTAs  
 294 (**1**), Scheme 1) could be employed as anchor, we chose  
 295 the catechol moiety because of its ability to chelate various  
 296 metal oxides ( $\text{HfO}_2$ ,  $\text{ZrO}_2$ ,  $\text{MnO}_2$ ,  $\text{Y}_2\text{O}_3$ ,  $\text{Al}_2\text{O}_3$ ,  $\text{TiO}_2$ ,  $\text{Fe}_2\text{O}_3$ ),  
 297 comparatively better pH stability of its complexes,<sup>40</sup> and  
 298 relatively mild procedure for its ligand exchange process.<sup>8,40,41</sup>

Since the trithiocarbonate moiety of RAFT agents is known to  
 decompose at elevated temperature,<sup>32</sup> Dopa-CTAs (**3a-c**) were  
 synthesized via amide linkages under mild conditions (Scheme  
 1).<sup>13,42</sup> This approach involved initial coupling of carboxyl CTAs  
 (**1a-c**) with a better leaving group (NHS) using EDC as the  
 carboxyl activating agent before amidization. NHS esters allow  
 efficient coupling with amines to yield amide bonds.<sup>42</sup> The  
 Dopa-CTAs (**3a-c**), termed Dopa-DDMAT, Dopa-DoPAT and  
 Dopa-CDSA respectively) were then prepared by reacting  
 dopamine with NHS-activated esters of the carboxylic RAFT  
 agents (**2a-c**). The formed compounds (**3a-c**) were confirmed  
 via 1D ( $^1\text{H}$  and  $^{13}\text{C}$ ) and 2D (gHSQC) NMR, ATR-FTIR, and UV-vis  
 spectroscopy.

$^1\text{H}$  NMR spectra of dopamine hydrochloride, DDMAT (**1a**), Suc-  
 DDMAT (**2a**), and Dopa-DDMAT (**3a**) are compared in Fig. 1.  
 The spectra show all the  $^1\text{H}$  peaks for the four compounds  
 (dopamine HCl, (**1a**), (**2a**) and (**3a**)), except the weak broad  
 carboxylic acid peak which is located at 10.73 ppm (for full  
 spectra of DDMAT (**1a**), see ESI Fig. S1†). With DDMAT (**1a**)  
 being converted into Suc-DDMAT (**2a**), this acid peak  
 disappears while a new peak 29, attributed to succinimidyl  
 protons, appears at 2.82 ppm. Further conversion of Suc-  
 DDMAT (**2a**) into Dopa-DDMAT (**3a**) was evident by the  
 absence of the peak 29 in the spectrum of Dopa-DDMAT (**3a**),  
 and the presence of new peaks 17-19, 21, 22, and 25. The peak  
 17 is the characteristic signal for the secondary amide proton,  
 while peaks 21, 22 and 25 are ascribed to the catechol  
 moiety.<sup>13,40,43</sup> It should be noted that the  $^1\text{H}$  peaks of phenol  
 hydroxyl groups 26 and 27 were absent when using  $\text{CDCl}_3$  as  
 solvent but would show when using  $\text{DMSO-d}_6$  as solvent.  $^{13}\text{C}$   
 NMR spectra of dopamine HCl, DDMAT (**1a**), Suc-DDMAT (**2a**),  
 and Dopa-DDMAT (**3a**) are compared in ESI Fig. S2.† The  
 synthesized Dopa-DDMAT (**3a**) was confirmed by the shifting  
 of the  $^{13}\text{C}$  carbonyl peak 16 and the presence of new  $^{13}\text{C}$  peaks  
 18 – 25 which are comparable to those of the dopamine HCl.

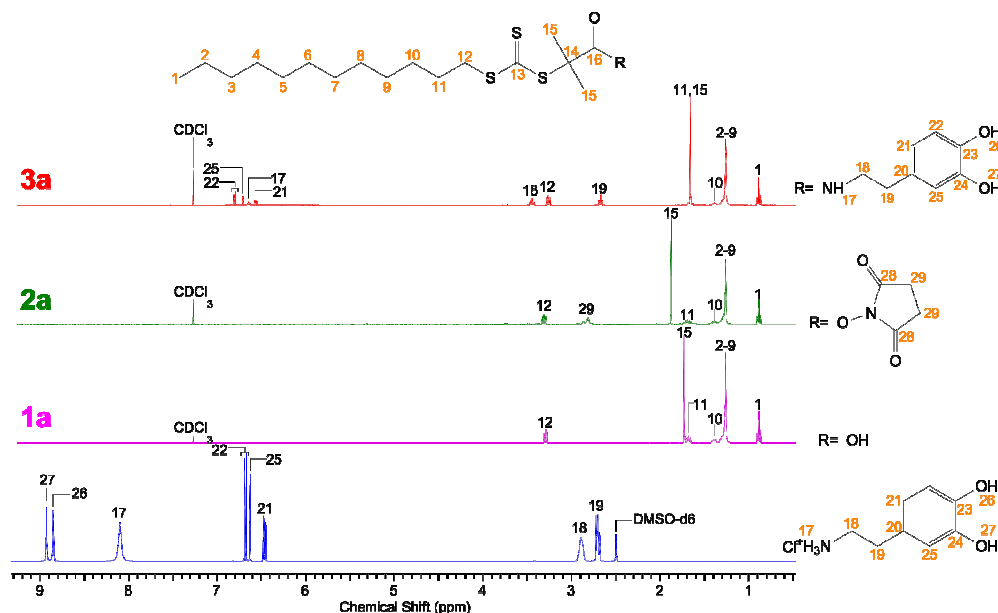


Figure 1.  $^1\text{H}$  NMR spectra of (bottom) dopamine hydrochloride, (**1a**) DDMAT, (**2a**) Suc-DDMAT, and (**3a**) Dopa-DDMAT (600 MHz, @  $25^\circ\text{C}$ ).

334 All the correlation  $^1\text{H}/^{13}\text{C}$  peaks for the synthesized Dopa-  
 335 DDMAT (**3a**) are clearly shown in ESI Fig S3<sup>+</sup>, confirming  
 336 peak assignments and molecular structure. Similarly, **3b**, **3c**  
 337 conversions of (**1b**) to (**2b**) then (**3b**), (**1c**) to (**2c**) and (**3c**)  
 338 also confirmed by their  $^1\text{H}$  and  $^{13}\text{C}$  NMR spectra in support  
 339 information (ESI Figs. S4 – S7<sup>+</sup>). The synthesized Dopa-  
 340 (**3a-c**) was also confirmed by ATR-FTIR investigation (ESI Figs.  
 341 S8 - S10<sup>+</sup>). Considering the UV wavelength range 320 to 380  
 342 nm for qualitative analysis, the trithiocarbonate group on  
 343 Dopa-CTAs (**3a-c**) was confirmed by the presence of a strong  
 344 absorption peak centred at 308-310 nm<sup>13</sup> while a shoulder  
 345 peak at 292-294 nm reveals the chromophoric effect of the  
 346 3,4-dihydroxyphenyl substituent (ESI Figs. S11 - S13<sup>+</sup>).

347 **Batch RAFT Polymerization of the Dopa-CTAs:** To investigate  
 348 the influence of the Dopa-CTAs over the growth of catechol  
 349 functionalized polyacrylamide (DPAM), RAFT polymerization of  
 350 acrylamide was carried out with a ratio of  $[\text{AM}]_0:[\text{Dopa-CTA}]_0:[\text{ACVA}]_0 = 2500:5:1$  at 70°C for each of the synthesized  
 351 Dopa-CTAs (**3a-c**), with the results listed in Table 1. Due to  
 352 poor noise-to-catechol signal ratios as the DPAM Mw increases,  
 353 the number-average Mw values via NMR analysis were only determined for 1hr DPAM samples and found to be  
 354 comparable with GPC measurements (ESI Table S1<sup>+</sup>). The RAFT  
 355 process was restricted to approximately 10 hr, since the cumulative radical activity of ACVA in DMSO is known to drop  
 356 drastically beyond 10 hr.<sup>26</sup> As seen in Fig. 2a, the number-  
 357 average molecular weights ( $M_{n,\text{GPC}}$ ) of DPAMs (**4a-c**)  
 358 synthesized using the three Dopa-CTAs (**3a-c**) increase with  
 359 increasing conversion of monomer AM while the dispersities  
 360 ( $\text{D}$ ) are very low,  $\leq 1.21$ , showing the characteristics of  
 361 living/controlled polymerization. More so, increased molecular  
 362 weight was evidenced by the shift in the GPC DRI peaks toward  
 363 shorter retention times (ESI Fig. S14<sup>+</sup>). Nonetheless, the  
 364 number-average molecular weights ( $M_{n,\text{GPC}}$ ) of the DPAM (**4a-**  
 365 **c**) overshoot their predicted values ( $M_{n,\text{theo}}$ ) with those of

**Table 1:** RAFT Polymerization of acrylamide mediated with Dopa-CTAs

Dopa-CTA ( <b>3</b> )	Time (min)	Conv. (%)	$M_{n,\text{GPC}}$	$M_{n,\text{theo}}^a$	$M_w$	$M_w/M_n$
(3a)	60	35.6	14800	13200	17600	1.19
	120	61.1	26200	22200	27300	1.04
	240	83.0	33700	30000	36100	1.07
	360	87.5	36300	31000	38900	1.07
	630	93.3	40700	33700	42700	1.05
(3b)	60	25.4	13900	9500	16800	1.21
	120	51.5	23800	18800	26100	1.10
	240	77.3	33100	28000	36500	1.10
	360	85.1	38000	30700	42900	1.13
	615	89.3	41000	32200	45700	1.12
(3c)	60	19.4	9400	7400	11300	1.21
	120	35.6	19600	13200	22100	1.13
	240	62.4	33300	22700	36800	1.10
	360	72.6	42400	26300	45900	1.08
	610	78.3	46300	28400	48500	1.05

Reaction conditions:  $[\text{AM}]_0:[\text{Dopa-CTA}]_0:[\text{ACVA}]_0 = 2500:5:1$ , solvent = 24.5 mL DMSO/DMF (97:3, vol%), Temp = 70°C,  $[\text{AM}]_0 = 2\text{M}$ . <sup>a</sup> $M_{n,\text{theo}} = \frac{M_w \times P}{[\text{AM}]_0} \times \frac{[\text{AM}]_0}{[\text{Dopa-CTA}]_0} \times \frac{[\text{Dopa-CTA}]_0}{[\text{AM}]_0}$  (where P is AM conversion,  $P=1-\frac{[\text{AM}]}{[\text{AM}]_0}$ ).

Dopa-CDSA (**4c**) giving the highest overshoot (Fig. 2a). Similar overshoots have been observed in a number of studies involving polymerization of acrylamide-based monomer mediated with trithiocarbonate RAFT agents,<sup>26,32,44</sup> with one of the plausible reasons for such discrepancy as explained by Thomas *et al.*<sup>23</sup> being the limited extent of utilization of the Dopa-CTAs.

The pseudo first order kinetic plots for AM polymerization using the Dopa-CTAs shown in Figure 2b deviate from linearity, approaching a polynomial distribution, thereby suggestive of

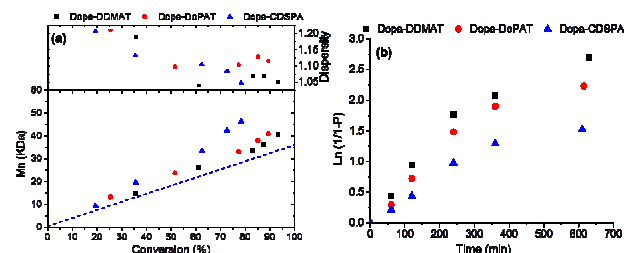
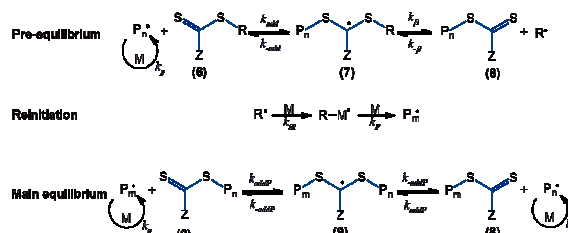
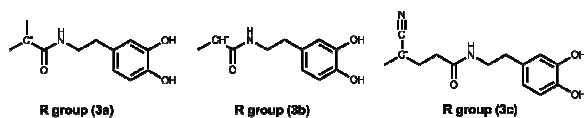


**Figure 2.** RAFT Polymerization of acrylamide mediated with Dopa-CTAs (**3a-c**) using  $[\text{M}]_0:[\text{CTA}]_0:[\text{I}]_0 = 2500:5:1$  ( $[\text{M}]_0 = 2\text{M}$ ), (a) evolution of molecular weight ( $M_n$ ) and dispersity with conversion (the theoretical  $M_n$  is represented with broken line ---); and (b) pseudo-first order kinetics, where P is AM conversion,  $P=1-[\text{AM}]/[\text{AM}]_0$ . Note: the theoretical  $M_n$  line slightly differs for each polymerization; however the lines overlap due to the insignificant difference in the MW of the Dopa-CTAs (**3a-c**).

the rate of propagation having non-steady state behaviour. This non-linearity may be explained by the change in cumulative radical production from ACVA in DMSO at 70°C owing to its decay constant.<sup>26</sup> Additional details on the cumulative radical production from ACVA in DMSO solvent as



**Scheme 2a.** RAFT Equilibria

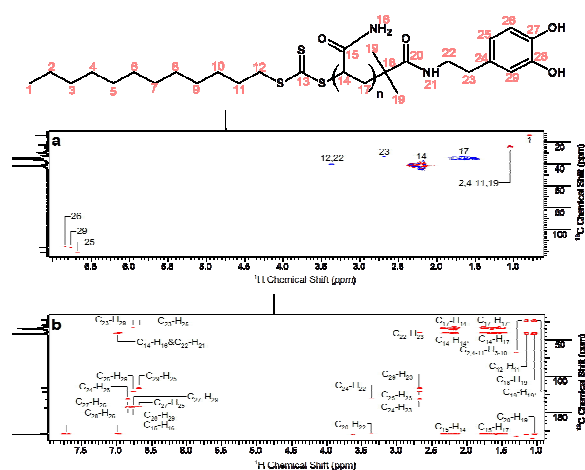


**Scheme 2b.** R group radicals of the Dopa-CTAs (**3**)

related to its decomposition rate constant at 70°C can be found in the literature.<sup>26</sup> More so, as identified by Moad and Barner-Kowollik,<sup>25</sup> the causes of non-steady state polymerization during the RAFT process include changing rate coefficients with chain length, slow fragmentation of RAFT adduct and large disparity in radical addition rates with respect to monomer and CTA. Cognizant of these causes, we dislodged the effect of the latter two by monitoring the rate of

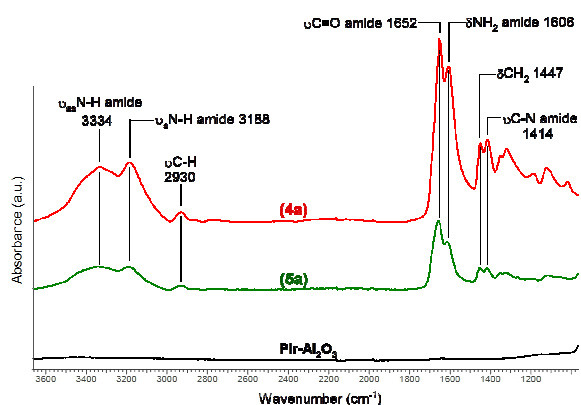
392 propagation after the pre-equilibrium period (i.e after 128  
 393 indicative of when the initial Dopa-CTAs had been completely  
 394 consumed, Figure 2b) to address the steady state assumption  
 395 of the propagating radicals  $[P_m^{\cdot}]$ . Overall, the Dopa-DDMAT  
 396 (3a) RAFT agent appears to have the most preferred living  
 397 characteristics based on its comparatively lower PDI values,  
 398 better linearity and lower extent of  $M_n$  overshoot (Fig. 2).  
 399 is expected since the catechol R groups must be generated  
 400 homolytic leaving groups and be capable of re-initiation, while  
 401 the ease of the former depending on the stability of the  
 402 corresponding expelled radicals (catechol R group derived).  
 403 The expelled radicals for both Dopa-DDMAT (3a) and Dopa-  
 404 CDSPA (3c) are tertiary, that of Dopa-DDMAT (3a) is stabilized  
 405 by two methyl groups and an electron donating carbonyl  
 406 carbon of amide group, while the other (3c) derived is  
 407 stabilized owing to the electron withdrawing effect of the  
 408 cyano group on its radical carbon center (See Scheme 2b).  
 409 expelled radical of Dopa-DoPAT (3b) is a secondary radical  
 410 stabilized by a methyl and an amide carbonyl. Steric effects  
 411 the catechol R groups were contributory to the stability of  
 412 their corresponding expelled radicals.<sup>24</sup>

413 **Alumina-PAM Nanocomposite:** The synthesized DPAM (4a)  
 414 prepared via RAFT polymerization ( $[AM]_0:[Dopa-CTA]_0:[ACVA]_0$   
 415 = 2500:5:1 at 70°C; duration = 35 min) was characterized with  
 416 1D ( $^1H$  and  $^{13}C$ ) and 2D (gHSQC, gHMBC) NMR. For the 1D NMR  
 417 spectra, see ESI Figs. S15 - S16†). As shown in Fig. 3 (gHSQC  
 418 and gHMBC spectra), all the correlation  $^1H/^{13}C$  peaks confirm  
 419 the peak assignments and the molecular structure of the  
 420 synthesized DPAM (4a). In addition to the major peaks (14, 16,  
 421 and 17) of the repeating unit of polyacrylamide, a few minor  
 422 peaks are present in the spectra of DPAM (4a). Peaks 1-12  
 423 suggest the presence of the Z' group ( $CH_3-(CH_2)_{11}-$ ) while peaks  
 424 19, 22-23, 25-26, and 29 indicate the presence of the  
 425 corresponding R group. The aromatic peaks 25, 26, and 29  
 426 confirm the catechol moiety in the synthesized DPAM. It  
 427 should be noted that the peak of trithiocarbonate carbon (13)



453 **Figure 3.** 2D (a) HSQC and (b) HMBC spectra of the synthesized  
 454 DPAM (4a) in  $D_2O$  @ 25°C.  $M_{n,NMR}$  of DPAM = 9313 g/mol  
 455 \*this proton is on the equivalent neighbouring carbon  
 456

is hardly seen in the  $^{13}C$  and gHMBC spectra in spite of an  
 extremely weak peak at 205 ppm which might be attributed to  
 it. Moreover, although there is no correlation  $^1H/^{13}C$  peak of  
 carbon 3 of the Z' group in the 2D NMR spectra, this carbon  
 peak is clearly seen in the  $^{13}C$  NMR spectrum at 31.9 ppm (ESI  
 Fig. S16†). With dopamine group being chemically attached to  
 the end of polyacrylamide chains, it was expected that the  
 catechol moiety could induce chemisorption of the polymer  
 onto the  $\gamma-Al_2O_3$  NP via covalent bonding or coordination  
 (mono- or bi-dentate bond).<sup>12,22</sup> The catechol group acts as the  
 adhesive moiety for mediating the nanocomposites formation  
 via the "grafting to" approach. The DPAM (4a) was selected for  
 anchoring to the pre-treated  $\gamma-Al_2O_3$ , since Dopa-DDMAT (3a)  
 appeared to be the most preferred CTAs for mediating AM  
 polymerization based on the estimated  $C_{tr}^{opp}$  and the  
 polymerization experiments. Fig. 4 shows the ATR-FTIR  
 spectrum of the dried  $\gamma-Al_2O_3$ -PAM PNC after extensive  
 washing, compared with those of the piranha-treated alumina  
 and DPAM (4a). While there is no significant peak in the  
 spectrum of the piranha-treated  $\gamma-Al_2O_3$  in the range of 1000-  
 3500  $cm^{-1}$ , the synthesized DPAM (4a) shows strong amide  
 peaks at 3334 (asymmetric N-H stretching), 3188 (symmetric  
 N-H stretching), 1652 (amide I C=O stretching), and 1606  $cm^{-1}$

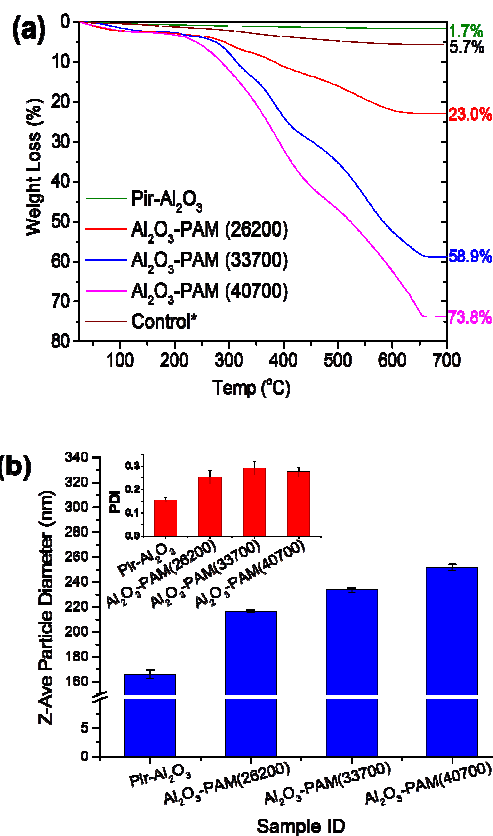


457 **Figure 4.** ATR-FTIR spectra of piranha-treated alumina (Pir- $Al_2O_3$ ),  
 458  $Al_2O_3$ -PAM (5a) and DPAM (4a).  
 459

451 (amide II N-H deformation and C-N stretching) in addition to  
 452 three minor peaks at 2930, 1447, and 1414  $cm^{-1}$  due to the C-H  
 453 stretching,  $CH_2$  bending, and C-N stretching vibrations,  
 454 respectively.<sup>46</sup> The presence of these amide and C-H peaks in  
 455 the spectrum of the synthesized  $Al_2O_3$ -PAM PNC indicates  
 456 successful attachment of the DPAM to the  $Al_2O_3$  NPs.

457 The attachment of DPAM on the surface of  $\gamma-Al_2O_3$  NPs was  
 458 also confirmed by TGA and DLS. Fig. 5a compares the weight  
 459 loss versus temperature for piranha-treated  $Al_2O_3$  NPs and  
 460  $Al_2O_3$ -PAM nanocomposites prepared using DPAM of different  
 461 molecular weights and PAM (without catechol moiety,  $M_{n,GPC}$  =  
 462 29600 Da) as a control. While the piranha-treated  $Al_2O_3$  lost  
 463 1.7% of weight when being heated to 700 °C, the control  
 464 sample lost 5.7% of weight, indicating 4% of physically  
 465 absorbed PAM. The  $Al_2O_3$ -PAM nanocomposites prepared  
 466 using DPAM of different molecular weights ( $M_n$  = 26200,

467 33700, and 40700 Da) demonstrated significantly high weight  
 468 losses of 23.0%, 58.9%, and 73.8%, respectively. The high  
 469 sensitivity in TGA weight loss with increased MW may be due  
 470 to the shorter polymer chains having enhanced interactions  
 471 with the alumina NPs. The hydrodynamic size of the PNCs was



472 **Figure 5.** Piranha-treated alumina and alumina-PAM (5a): (a) thermo-gravimetric analysis, and (b) dynamic light scattering analysis.  
 473 \* $\gamma$ -Al<sub>2</sub>O<sub>3</sub> chemisorbed with PAM (without catechol moiety,  $M_{n,GPC}$  = 29600 Da)

472 assessed using the Z-average hydrodynamic diameter  
 473 instead of average  $D_h$ . The Z-average value which is based on  
 474 cummulant method was used as a criterion for comparison  
 475 because it is numerically stable and less sensitive to noise  
 476 compared to average  $D_h$ .<sup>47</sup> The Z-average  $D_h$  values for  
 477 Al<sub>2</sub>O<sub>3</sub>, Al<sub>2</sub>O<sub>3</sub>-PAM (26200 Da), Al<sub>2</sub>O<sub>3</sub>-PAM (33700 Da)  
 478 Al<sub>2</sub>O<sub>3</sub>-PAM (40700 Da) were measured to be 165.8, 233.6,  
 479 251.5 and 251.5 nm, respectively, with each having a width  
 480 parameter  $\leq 0.3$  (Fig. 5b). Comparison of the hydrodynamic  
 481 size and PDI ( $=\sigma/d^2$ ) of the Al<sub>2</sub>O<sub>3</sub>-PAM PNCs with the bare  
 482 Al<sub>2</sub>O<sub>3</sub> is indicative of good dispersivity of the PNC in water  
 483 (where,  $\sigma$  = standard deviation,  $d$  = average diameter).  
 484 expected, the Z-ave size of the Al<sub>2</sub>O<sub>3</sub>-PAM increased with  
 485 length of the polymer chains.

486 This study indicates that the catechol end-group CTAs provide  
 487 a suitable route for end-functionalization of PAM for post-  
 488 modification chemistry. Furthermore, RAFT agents with R

groups bearing catechol polar ends provide good stability for controlled polymerization.

## Conclusions

492 In order to produce stable tethering to metal oxide  
 493 nanoparticles, three novel catechol end trithiocarbonate CTAs  
 494 (Dopa-CTAs) which differ in their carbonyl  $\alpha$ -substituents were  
 495 synthesized and their molecular structures were confirmed by  
 496 NMR, UV-Vis and ATR-FTIR. The Dopa-CTAs were all found to  
 497 mediate homo-polymerization of acrylamide in a controlled  
 498 and quantitative fashion, and the Dopa-DDMAT was found to  
 499 be the most preferred based on the livingness characteristics  
 500 and its structural constituents. As evident from the binding  
 501 studies with  $\gamma$ -Al<sub>2</sub>O<sub>3</sub> NPs, catechol end-group CTAs provide a  
 502 suitable route for end-functionalization of PAM to allow post-  
 503 modification chemistry aimed at synthesizing PNCs.

## Acknowledgements

504 The authors acknowledge Polyanalytik Inc. Ontario for  
 505 providing the PEO standards used for calibrating the GPC  
 506 instrument. We also thank Prof. John R. de Bruyn (Western  
 507 University) and his group for granting us access to use the  
 508 refractometer in their facility. Funding was provided by  
 509 Canada's National Science & Engineering Research Council  
 510 (NSERC) Discovery program.

## Notes and references

- 513 1. Y. Wang, Y. Kotsuchibashi, Y. Liu and R. Narain, *Langmuir*, 2014, **30**, 2360-2368.
- 514 2. S. Ji and J. Y. Walz, *The Journal of Physical Chemistry B*, 2013, **117**, 16602-16609.
- 515 3. J.-P. O'Shea, G. G. Qiao and G. V. Franks, *Journal of Colloid and Interface Science*, 2011, **360**, 61-70.
- 516 4. R. Pamies, K. Zhu, S. Volden, A.-L. Kjoniksen, G. Karlsson, W. R. Glomm and B. Nystrom, *Journal of Physical Chemistry C*, 2010, **114**, 21960-21968.
- 517 5. *US Pat.*, 20120138543, 2012.
- 518 6. G. Rytwo, R. Lavi, Y. Rytwo, H. Monchase, S. Dultz and T. N. König, *Science of The Total Environment*, 2013, **442**, 134-142.
- 519 7. S. Wang, M.Sc. Thesis, University of Alberta (Canada), 2013.
- 520 8. B. Hojjati, R. Sui and P. A. Charpentier, *Polymer*, 2007, **48**, 5850-5858.
- 521 9. H. Lee, N. F. Scherer and P. B. Messersmith, *Proceedings of the National Academy of Sciences*, 2006, **103**, 12999-13003.
- 522 10. H. Lee, S. M. Dellatore, W. M. Miller and P. B. Messersmith, *Science*, 2007, **318**, 426-430.
- 523 11. E. Amstad, T. Gillich, I. Bilecka, M. Textor and E. Reimhult, *Nano Letters*, 2009, **9**, 4042-4048.
- 524 12. W. O. Yah, H. Xu, H. Soejima, W. Ma, Y. Lvov and A. Takahara, *Journal of the American Chemical Society*, 2012, **134**, 12134-12137.



- 540 13. C. Zobrist, J. Sobocinski, J. Lyskawa, D. Fournier, V. 602  
 541 M. Traisnel, M. Jimenez and P. Woisel, *Macromolecules*, 2011, **44**, 5883-5892. 603  
 542 604  
 543 14. P. H. Mutin, G. Guerrero and A. Vioux, *Journal of* 605  
 544 *Materials Chemistry*, 2005, **15**, 3761-3768. 606  
 545 15. C. Li and B. C. Benicewicz, *Journal of Polymer Science* 607  
 546 *A: Polymer Chemistry*, 2005, **43**, 1535-1543. 608  
 547 16. C. Li, J. Han, C. Y. Ryu and B. C. Benicewicz, *Macromolecules*, 2006, **39**, 3175-3183. 609  
 548 610  
 549 17. C. Yang, R. Jie, L. Jianbo and L. Yan, *Materials Letters* 611  
 550 2010, **64**, 1570-1573. 612  
 551 18. C. Boyer, M. R. Whittaker, V. Bulmus, J. Liu and T. P. Davis, 613  
 552 *NPG Asia Mater*, 2010, **2**, 23-30. 614  
 553 19. B. S. Sumerlin, A. B. Lowe, P. A. Stroud, P. Zhang, M. 615  
 554 Urban and C. L. McCormick, *Langmuir*, 2003, **19**, 5506-5562. 616  
 555 617  
 556 20. O. Yilmaz, M. Karesoja, A. C. Adiguzel, G. Zengin and 618  
 557 Tenhu, *Journal of Polymer Science Part A: Polymer Chemistry*, 2014, **52**, 1435-1447. 619  
 558 620  
 559 21. M. B. McBride and L. G. Wesselink, *Environmental Science & Technology*, 1988, **22**, 703-708. 621  
 560 622  
 561 22. J. H. Waite and M. L. Tanzer, *Science*, 1981, **212**, 1023-1040. 623  
 562 624  
 563 23. J. Krstina, G. Moad, E. Rizzardo, C. L. Winzor, C. T. Berge 625  
 564 and M. Fryd, *Macromolecules*, 1995, **28**, 5381-5385. 626  
 565 24. L. Barner and S. Perrier, in *Handbook of RAFT polymerization*, ed. C. Barner-Kowollik, Wiley-VCH, Weinheim, 2008, pp. 455-482. 627  
 566 628  
 567 25. G. Moad and C. Barner-Kowollik, in *Handbook of RAFT polymerization*, ed. C. Barner-Kowollik, WILEY-VCH, Weinheim, 2008, pp. 51-104. 629  
 568 630  
 569 26. D. B. Thomas, A. J. Convertine, L. J. Myrick, C. W. Scales, A. 631  
 570 E. Smith, A. B. Lowe, Y. A. Vasilieva, N. Ayres and C. L. McCormick, *Macromolecules*, 2004, **37**, 8941-8950. 632  
 571 633  
 572 27. M. Arslan, T. N. Gevrek, J. Lyskawa, S. Szunerits, R. Boukherroub, R. Sanyal, P. Woisel and A. Sanyal, *Macromolecules*, 2014, **47**, 5124-5134. 634  
 573 635  
 574 28. J. S. Kim, T. G. Kim, W. H. Kong, T. G. Park and Y. S. Nam, *Chemical Communications*, 2012, **48**, 9227-9229. 636  
 575 637  
 576 29. Y. Min and P. T. Hammond, *Chemistry of Materials*, 2011, **23**, 5349-5357. 638  
 577 639  
 578 30. D. J. Keddie, G. Moad, E. Rizzardo and S. H. Thang, *Macromolecules*, 2012, **45**, 5321-5342. 640  
 579 641  
 580 31. J. Lee, O. Kim, S. Shim, B. Lee and S. Choe, *Macromol. Res.*, 2005, **13**, 236-242. 642  
 581 643  
 582 32. A. J. Convertine, B. S. Lokitz, A. B. Lowe, C. W. Scales, L. J. Myrick and C. L. McCormick, *Macromolecular Rapid Communications*, 2005, **26**, 791-795. 644  
 583 645  
 584 33. W. Sun, J. Long, Z. Xu and J. H. Masliyah, *Langmuir*, 2008, **24**, 14015-14021. 646  
 585 647  
 586 34. W. Y. Yang, J. W. Qian and Z. Q. Shen, *Journal of Colloid and Interface Science*, 2004, **273**, 400-405. 648  
 587 649  
 588 35. A. R. Barron, *Dalton Transactions*, 2014, **43**, 8127-8143. 650  
 589 651  
 590 36. B. Kasprzyk-Hordern, *Advances in Colloid and Interface Science*, 2004, **110**, 19-48. 652  
 591 653  
 592 37. H. Gulley-Stahl, P. A. Hogan, W. L. Schmidt, S. J. Wall, A. Buhrlage and H. A. Bullen, *Environmental Science & Technology*, 2010, **44**, 4116-4121. 654  
 593 655  
 594 38. G. S. Tulevski, Q. Miao, M. Fukuto, R. Abram, B. Ocko, R. Pindak, M. L. Steigerwald, C. R. Kagan and C. Nuckolls, *Journal of the American Chemical Society*, 2004, **126**, 15048-15050. 656  
 595 657  
 596 39. V. S. Wilms, H. Bauer, C. Tonhauser, A.-M. Schilman, M.-C. Müller, W. Tremel and H. Frey, *Biomacromolecules*, 2013, **14**, 193-199. 658  
 597 659  
 598 40. H. B. Na, G. Palui, J. T. Rosenberg, X. Ji, S. C. Grant and H. Mattoussi, *ACS Nano*, 2012, **6**, 389-399. 660  
 599 661  
 600 41. H. Comas, V. Laporte, F. Borcard, P. Miéville, F. Krauss Juillerat, M. A. Caporini, U. T. Gonzenbach, L. Juillerat-Jeanneret and S. Gerber-Lemaire, *ACS Applied Materials & Interfaces*, 2012, **4**, 573-576. 662  
 601 663  
 602 42. E. Valeur and M. Bradley, *Chemical Society Reviews*, 2009, **38**, 606-631. 664  
 603 665  
 604 43. A. Isakova, P. D. Topham and A. J. Sutherland, *Macromolecules*, 2014, **47**, 2561-2568. 666  
 605 667  
 606 44. M. Hernandez-Guerrero, E. Min, C. Barner-Kowollik, A. H. E. Muller and M. H. Stenzel, *Journal of Materials Chemistry*, 2008, **18**, 4718-4730. 668  
 607 669  
 608 45. M. L. Coote and D. J. Henry, *Macromolecules*, 2005, **38**, 1415-1433. 670  
 609 671  
 610 46. L. T. Chiem, L. Huynh, J. Ralston and D. A. Beattie, *Journal of Colloid and Interface Science*, 2006, **297**, 54-61. 672  
 611 673  
 612 47. ISO. 22412:2008, *Particle size analysis – photon correlation spectroscopy*, International Organization for Standardization, Geneva, Switzerland, 2008. 674  
 613 675